# Guanine Oxidation: NMR Characterization of a Dehydro-guanidinohydantoin Residue Generated by a 2e-oxidation of d(GpT)

**Arkadiusz Chworos,† Yannick Coppel, Igor Dubey,‡ Geneviève Pratviel,* and Bernard Meunier***

*Contribution from the Laboratoire de Chimie de Coordination du CNRS, 205 route de Narbonne, 31077 Toulouse Cedex 4, France.*

*Received November 13, 2000*

**Abstract:** The Mn-TMPyP/$KHSO_5$ system was used to oxidize guanine contained within a dinucleoside monophosphate **d(GpT)**. To identify the guanine oxidation product having a mass with 4 amu above the mass of guanine itself, this relatively unstable compound was reduced to a more stable one. The ESI/MS and NMR data allowed us to propose a dehydro-guanidinohydantoin structure for the **(G+4)** guanine oxidation product.

## Introduction

DNA oxidation is a field of intense interest due to the deleterious effects that oxidative damage promotes within cells.[1−7] Guanine is the most oxidizable base and constitutes the main target of oxidants. The cationic metalloporphyrin, manganese(III)−bis(aqua)-*meso*-tetrakis(4-*N*-methylpyridiniumyl)-porphyrin, Mn−TMPyP, activated by $KHSO_5$ into a high-valent metal−oxo species ($Mn^V$═O) is able to oxidize guanine bases by a two-electron abstraction mechanism.[8] On the basis of HPLC coupled with electrospray ionization mass (ESI/MS) analyses, it was possible to observe different guanine oxidation products generated by Mn−TMPyP/$KHSO_5$ on short double-stranded G-rich oligonucleotides.[9] Using this method, these oxidative lesions could be analyzed immediately after the reaction was carried out at 0 °C, without any further workup. They can be considered as primary lesions and thus as potentially biological relevant lesions. On these double-stranded DNA models, the major product of guanine oxidation was proposed to be an oxidized guanidinohydantoin. Since the products of guanine oxidation were only analyzed by mass spectrometry, it was referred to as the **(G+4)** residue since its mass corresponded to 4 amu above that of guanine. A dehydro-guanidinohydantoin structure was proposed for the **(G+4)** compound (structure **1**, Figure 1) on the basis of a general mechanism of guanine oxidation where **(G+4)** was postulated to be an immediate precursor of imidazolone, a known product of guanine oxidation by electron transfer.[10] However, two **(G+4)** compounds could be, in theory, on the route of imidazolone (**1** and **2**, Figure 1) as initially proposed.[8] We favored the dehydro-guanidinohydantoin structure (**1**) because it should form first according to the proposed general mechanism of guanine oxidation and should be stabilized by hydrogen bonding with the complementary cytosine within double-stranded DNA.[8,9] Recently, a third **(G+4)** compound was reported (**3** in Figure 1) as main oxidation product of 8-oxo-7,8-dihydro-2′-deoxyguanosine by peroxynitrite.[11a] A structure reminiscent of **1** was proposed later by the same authors for a nitration product of 8-oxo-7,8-dihydro-2′-deoxyguanosine under oxidation by peroxynitrite.[11b] The dehydro-guanidinohydantoin lesion **(G+4)** may also be generated as the main singlet oxygen oxidation product of 8-oxo-7,8-dihydroguanine within single-stranded oligonucleotides.[12] We decided to further investigate the structure corresponding to the observed **(G+4)** lesion generated by Mn−TMPyP/$KHSO_5$ among the three different possible structures **1**−**3** (Figure 1).

In the present work, we used a dinucleotide derivative, the dinucleoside monophosphate **d(GpT)**, as a simplified DNA model, to isolate the **(G+4)** compound in large amount and to characterize it by NMR spectroscopy. The oxidation of **d(GpT)** by Mn−TMPyP/$KHSO_5$ led to two oxidation products: the imidazolone containing dinucleotide, **d(IzpT)** and the **d(G+4pT)** derivative. The latter could not be analyzed directly since it was unstable. It was transformed into an oxaluric acid derivative. Due to this unstability, **d(G+4pT)** was reduced into a stable derivative before NMR analyses.[11] The reduction of **d(G+4pT)** gave a mixture of two compounds with molecular masses corresponding to an increase of 2 amu

† Present address: Department of Bioorganic Chemistry, Center of Molecular and Macromolecular Studies, Polish Academy of Sciences, Lodz, Poland.

‡ Institute of Molecular Biology and Genetics, National Academy of Sciences, Kiev, Ukraine.

(1) Demple, B.; Harrison, L. *Annu. Rev. Biochem.* **1994**, *63*, 915−948.
(2) von Sonntag, C. In *The Chemical Basis of Radiation Biology;* Taylor and Francis: London, 1987.
(3) Burrows, C. J.; Muller, J. G. *Chem. Rev.* **1998**, *98*, 1109−1151.
(4) Pratviel, G.; Bernadou, J.; Meunier, B. *Angew. Chem., Int. Ed. Engl.* **1995**, *34*, 746−769.
(5) Pratviel, G.; Bernadou, J.; Meunier, B. *Adv. Inorg. Chem.* **1997**, *45*, 251−312.
(6) Breen, A. P.; Murphy, J. A. *Free Rad. Biol. Med.* **1995**, *18*, 1033−1077.
(7) Cadet, J.; Berger, M.; Douki, T.; Ravanat, J.-L. *Rev. Physiol. Biochem. Pharmacol.* **1997**, *131*, 1−87.
(8) Vialas, C.; Pratviel, G.; Claparols, C.; Meunier, B. *J. Am. Chem. Soc.* **1998**, *120*, 11548−11553.
(9) Vialas, C.; Claparols, C.; Pratviel, G.; Meunier, B. *J. Am. Chem. Soc.* **2000**, *122*, 2157−2167.
(10) Cadet, J.; Berger, M.; Buchko, G. W.; Joshi, P. C.; Raoul, S.; Ravanat, J.-L. *J. Am. Chem. Soc.* **1994**, *116*, 7403−7404.
(11) (a) Niles, J. C.; Burney, S.; Singh, S. P., Wishnok, J. S.; Tannenbaum, S. R. *Proc. Natl. Acad. Sci. U.S.A.*, **1999**, *96*, 11729−11734. (b) Niles, J. C.; Wishnok, J. S.; Tannenbaum, S. R. *Chem. Res. Toxicol.*, **2000**, *13*, 390−396.
(12) Duarte, V.; Gasparutto, D.; Yamaguchi, L. F.; Ravanat, J.-L.; Martinez, G. R.; Medeiros, M. H. G.; Di Mascio, P.; Cadet, J. *J. Am. Chem. Soc.* **2000**, *122*, 12622−12628.

10.1021/ja003945p CCC: $20.00 
Published on Web 06/05/2001

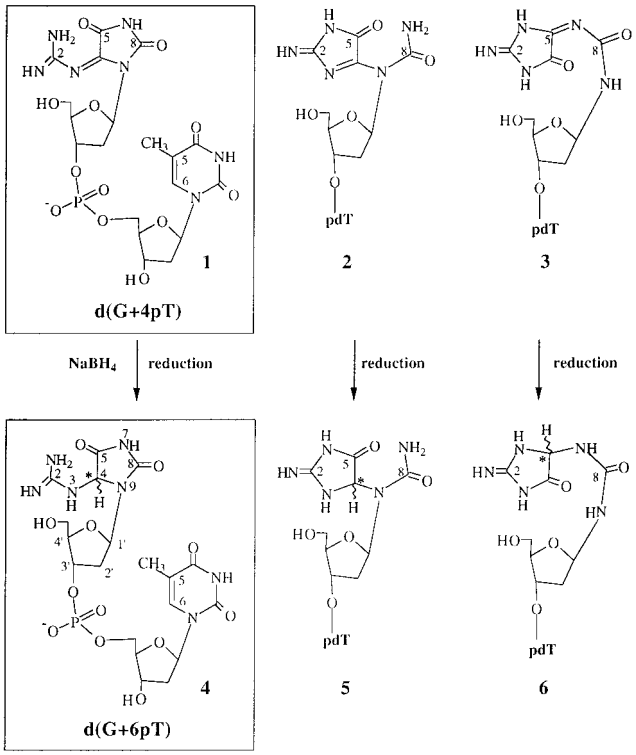


**Figure 1.** Three possible structures for the guanine oxidation compound **(G+4)** on the **d(GpT)** substrate. Reduction of **d(G+4pT)** by $NaBH_4$ leads to **d(G+6pT)**. Note that * indicates a chiral center. The numbering of the carbon atoms refers to the one of the initial guanine. The highlighted structures correspond to the ones proposed for **d(G+4pT)** and **d(G+6pT)** in the present work.

compared to **d(G+4pT)** and thus to 6 amu compared to the initial mass of **d(GpT)**. They were referred to as **d(G+6pT)** derivatives in the text. The three **(G+4)** structures **1**, **2**, and **3** of Figure 1 could be reduced to generate the corresponding **d(G+6pT)** reduction products **4**, **5**, and **6**. However, from mass fragmentation and NMR data, we propose that the two **d(G+6pT)** products observed in the present work correspond to the two diastereoisomers of a guanidinohydantoin residue **(G+6)** (compound **4**, Figure 1). From the characterization of these two **d(G+6pT)** isomers, it was thus possible to confirm the structure of the **d(G+4pT)** derivative as the dehydro-guanidinohydantoin derivative **1** (Figure 1). Moreover, we found that the dehydro-guanidinohydantoin **(G+4)** was not a precursor of imidazolone as previously proposed.[9] It is rather the precursor of an oxaluric acid derivative probably through an intermediate parabanic acid derivative.[11,12]

## Results

**1. Oxidation of d(GpT) by Mn−TMPyP/$KHSO_5$.** Since guanine oxidation leads to a decrease of the UV absorbance and an increase in the polarity of the products, we decided to study the guanine oxidation reaction with a dinucleoside monophosphate substrate, **d(GpT)**. This allowed us to easily monitor the reaction by reverse phase HPLC coupled to a diode array UV−visible detector. The UV absorbance of thymine, which remains untouched during the oxidation reaction, was useful for the UV detection. The dinucleotide derivatives eluted at a higher retention time on reverse phase column compared to mononucleoside ones. Therefore, the oxidized compounds could be separated and isolated.

The oxidation of **d(GpT)** by Mn−TMPyP/$KHSO_5$ led to two oxidation products after 5 min at 0 °C (Figure 2). The reaction was stopped by the addition of HEPES buffer which reacts with the excess of $KHSO_5$. The reaction mixture was analyzed by HPLC-ESI/MS. The HPLC trace is shown in Figure 2A (detection 260 nm). The two oxidation products were attributed to an imidazolone-modified dinucleotide, **d(IzpT)**, at 26.8 min and a dinucleotide carrying an oxidized guanidinohydantoin moiety, **d(G+4pT)**, at 23.5 min from their molecular masses. The residual **d(GpT)** eluted at 30.9 min. The observed mono-charged $[M - H]^-$ ions at *m*/*z* 570.1, 531.1, and 573.9 corresponded to **d(GpT)**, **d(IzpT)**, and **d(G+4pT)**, respectively. The UV−vis spectra of the two oxidation products of **d(GpT)** are shown in Figure 2B and are different from the UV-spectrum of **d(GpT)**. The $\lambda_{max}$ for **d(IzpT)** were at 258 and 325 nm, and for **d(G+4pT)** at 238 nm. It must be noted that with this simplified DNA model, as also observed in the case of nucleosides, the **(G+4)** modified base lesion was not the major guanine oxidation product, whereas it is the main oxidation product of guanine for double-stranded oligonucleotides.[9] After the oxidation reaction was stopped by the addition of HEPES buffer, the half-life of **d(G+4pT)** was found to be 8 h in the reaction triethylammonium acetate buffer (TEAA buffer pH 6.5 at 0 °C). This relative stability is not compatible with this compound being an immediate precursor of **d(IzpT)**, since **d(IzpT)** is formed within a few minutes.

The next step was to carry out this reaction on a larger scale to isolate the oxidation products for NMR analysis. The imidazolone-modified dinucleotide was stable enough to undergo collection of the HPLC peak followed by lyophilization of fractions provided the samples were kept at low temperature (no heating during speed-vac lyophilization). The NMR data for **d(IzpT)** is described in Table S1 in the Supporting Information. However, partial degradation of **d(IzpT)** during the purification process was observed since the product did not appear as 100% pure on the $^1H$ NMR analysis (10−20% of a byproduct). The other oxidation product, **d(G+4pT)** proved to be unstable under the used HPLC purification protocol, and thus its isolation was not possible by using that method.

**2. Unstability of d(G+4pT).** The main degradation product of the **d(G+4pT)** compound when isolation was carried out from HPLC collection followed by speed-vac procedure was a compound with a $[M - H]^-$ molecular mass signal at *m*/*z* 551.0, corresponding to a **d(G-19pT)** product. We observed that this degradation product was also the main product of degradation of the **(G+4)** lesion upon heating at 90 °C in water (data not shown). The fact that **d(G+4pT)** did not transform into **d(IzpT)** showed again that **d(G+4pT)** was not a precursor of **d(IzpT)**. The ESI/MS/MS analysis of the **d(G-19pT)** compound is shown in Figure S2. The main fragments observed from the 551 amu ion corresponded to *m*/*z* signals at 479.1, 436.2, and 320.9 amu. This fragmentation is the same as the one recently reported for an oxaluric acid derivative obtained from the oxidation of 8-oxo-guanine by singlet oxygen.[12] From this MS/MS fragmentation the **(G-19)** modified residue was tentatively attributed to a "linear" oxaluric acid derivative that might be formed through a parabanic acid intermediate[9] due to the hydrolysis of structure **1** and not of structure **2** for **d(G+4pT)** (Figure 1). This oxaluric acid derivative was considered not to be informative enough for the NMR determination of the structure of the **d(G+4pT)** compound, while we found that the reduction of **d(G+4pT)** with $NaBH_4$ into a stable species proved to be the method of choice for the characterization of the **(G+4)** lesion on **d(GpT)**.

**3. Reduction of d(G+4pT) by $NaBH_4$ Leads to Two d(G+6pT) Isomers.** After isolation of the **d(G+4pT)** from the reaction medium by HPLC purification, immediate $NaBH_4$

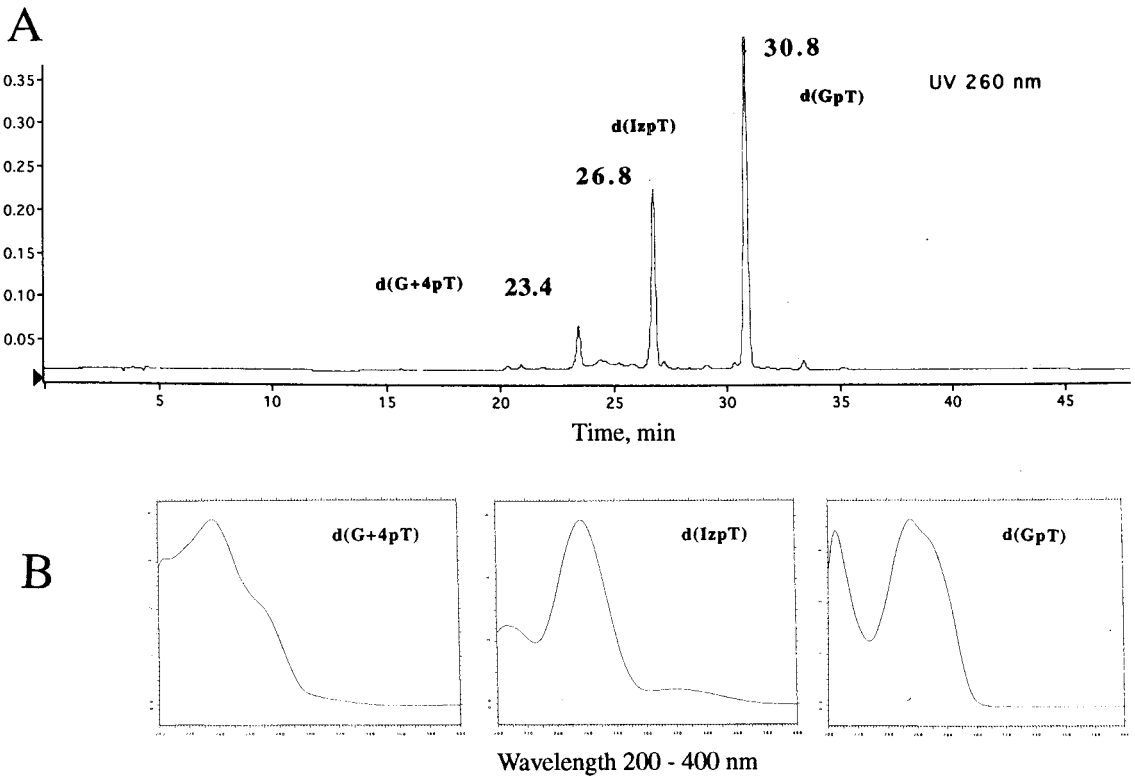


**Figure 2.** HPLC-ESI/MS analysis of the oxidation of **d(GpT)** by Mn-TMPyP/$KHSO_5$. (A) Reverse phase HPLC trace of the oxidation of **d(GpT)** by Mn-TMPyP/$KHSO_5$ (A). The chromatographic conditions corresponded to gradient A. Detection is at 260 nm. On-line UV−vis analyses of the HPLC peaks (B).

reduction before any further workup was performed. The reduction was quantitative after 30 min at room temperature. Two products which eluted before the initial **d(G+4pT)** compound were obtained. The HPLC-ESI/MS analyses of the mixture of the two products of reduction are shown in Figure 3 (eluting conditions being different from that of Figure 2, retention times are not comparable). The UV detection chart (260 nm) is shown in the upper part (Figure 3A) and the on-line UV−vis spectra corresponding to the two HPLC peaks in Figure 3B. The ratio of the two products was 35/65 (fast-/slow-eluting one). The ratio of the two **d(G+6pT)** products was estimated from their HPLC peak areas since they showed the same UV absorbance ($\lambda_{max}$ = 270 nm) (Figure 3B). The mass spectra of the two peaks, eluting at 28 ("fast") and 29.7 min ("slow"), were similar and showed a $[M - H]^-$ signal at *m*/*z* 576.1. The two compounds of the reduction reaction showed an increase of 2 amu compared to the **d(G+4pT)** derivative whose monocharged $[M - H]^-$ ion was at *m*/*z* 573.9. They were thus referred to as **d(G+6pT)** slow- and fast-eluting derivatives, according to their relative retention times. The two compounds exhibited the same fragmentation behavior during electrospray ionization analyses, leading to a signal at *m*/*z* 517.2 corresponding to a loss of 59 amu from the molecular mass. This fragmentation can be interpreted by the loss of a molecule of guanidine followed by the loss of one proton.

The two **d(G+6pT)** compounds transformed one into the other. Although they were collected separately, HPLC as well as NMR analyses showed that they could not be obtained as pure samples but always as a mixture of both isomers. After 2 h of incubation at ambient temperature in triethylammonium acetate buffer pH 6.5, the fast-eluting compound (collected as a single product) appeared as a mixture of 60/40, fast-/slow-eluting derivatives, according to the HPLC analysis. The slow-eluting compound, under the same conditions, gave an HPLC profile of a mixture of 35/65 of the fast-/slow-eluting derivatives. The conversion of the fast-eluting isomer into the slow-eluting one was always more rapid than the opposite conversion. Both mixtures however tended to an equilibrium consisting of 35% of the fast- and 65% of the slow-eluting compound. This corresponded to the ratio obtained after the reduction reaction. In summary, the reduction products of **d(G+4pT)** consisted of a mixture of two **d(G+6pT)** isomers with the slow-eluting compound (65%) as the slightly thermodynamically favored species. The slow- and fast-eluting isomers were also referred to as the major and minor ones, respectively. The isomerization process will be discussed in the Discussion.

**4. Stability of d(G+6pT) isomers. 4.1. Stability of d(G+6pT) upon heating.** Incubation of the 35/65 (fast-/slow-eluting) mixture of **d(G+6pT)** isomers at 90 °C in neutral pH buffered solution for 30 min showed that the two compounds were perfectly stable. The ratio of the two HPLC peaks remained unchanged during that treatment.

**4.2. Piperidine Treatment of d(G+6pT).** The two isomers of **d(G+6pT)** were equally sensitive to piperidine. Upon incubation of a 35/65 mixture of isomers of **d(G+6pT)**, in 1 M piperidine, at 90 °C during 30 min, the two compounds were transformed into thymidine 5′-monophosphate as deduced from the co-injection with the standard product. The reaction was complete. Thymidine-5′-monophosphate was the only product detected on the HPLC trace at 260 nm. The area of the HPLC peak of thymidine-5′-monophosphate corresponded to that of the initial two **d(G+6pT)** compounds which is consistent with the released **(G+6)** not contributing significantly to UV absorbance.

**5. Reoxidation of d(G+6pT) Isomers.** Incubation of the mixture of isomers of **d(G+6pT)** with a catalytic amount of Mn−TMPyP/$KHSO_5$ gave rise to a preferential oxidation of the sugars of the dinucleotide derivative instead of reoxidation

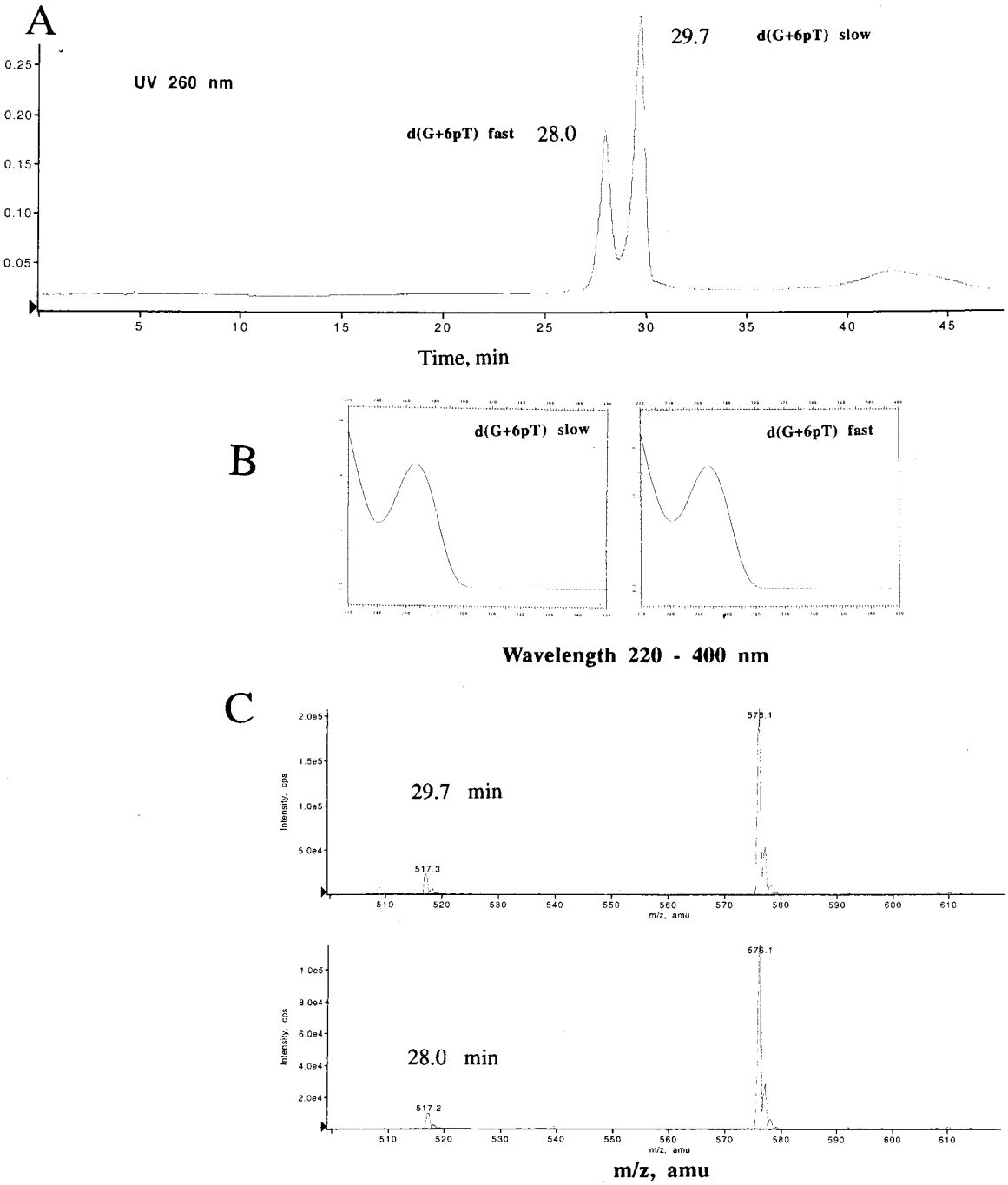


**Figure 3.** HPLC-ESI/MS analysis of the two isomers of **d(G+6pT)**. The chromatographic conditions corresponded to gradient B. HPLC trace (A), on-line UV−visible (B) and on-line ESI/MS analyses of the HPLC peaks (C).

of the modified base. The mixture of **d(G+6pT)** isomers was totally degradated within 15 min at room temperature (not shown). This is due to the high reactivity of the oxo-metalloporphyrin toward the sugars[4,5] that are more accessible in the case of a dinucleotide derivative compared to a double-stranded DNA substrate. However, we found that it was possible to oxidize **d(G+6pT)** isomers to the **d(G+4pT)** compound by reaction with a milder oxidant, the 1,2-naphthoquinone-4-sulfonate (NQS). The HPLC-ESI/MS analysis of this reaction is reported in Table 1 and Figure 4. The mixture of **d(G+6pT)** isomers (100 $\mu$M) was incubated with NQS (200 $\mu$M) in water. After 10 min at room temperature no reaction occurred. Increasing the temperature to 65 °C promoted the appearance of a new product with the same retention time and the same on-line mass spectrum as **d(G+4pT)** after 5 min ($m/z$ = 574.1 amu) (Figure 4A and Table 1). As shown in Figure 4B, further incubation at 65 °C for 30 min promoted the appearance of

**Table 1.** HPLC/ESI-MS Data of Oxidation of **d(G+6pT)** by NQS after 30 min at 65 °C (see also Figure 4B)

| $m/z$ | $\Delta M$[a] | $R_t$ (min)[b] | proposed structure for G lesion |
|---|---|---|---|
| 576.1 | 6 | 28 | **d(G+6pT)** |
| 517.2 | | | fragmentation |
| 576.2 | 6 | 29.6 | **d(G+6pT)** |
| 517.3 | | | fragmentation |
| 574.1 | 4 | 33.2 | **d(G+4pT)** |
| 551.0 | −19 | 37.5 | **d(G-19pT)** |
| 436.3 | | | fragmentation |
| 533.2 | - | 43.1 | **d(G-37pT)** |

[a] $\Delta M$: mass of the modified product minus the mass of the initial **d(GpT)**. [b] Gradient B (see Experimental Section).

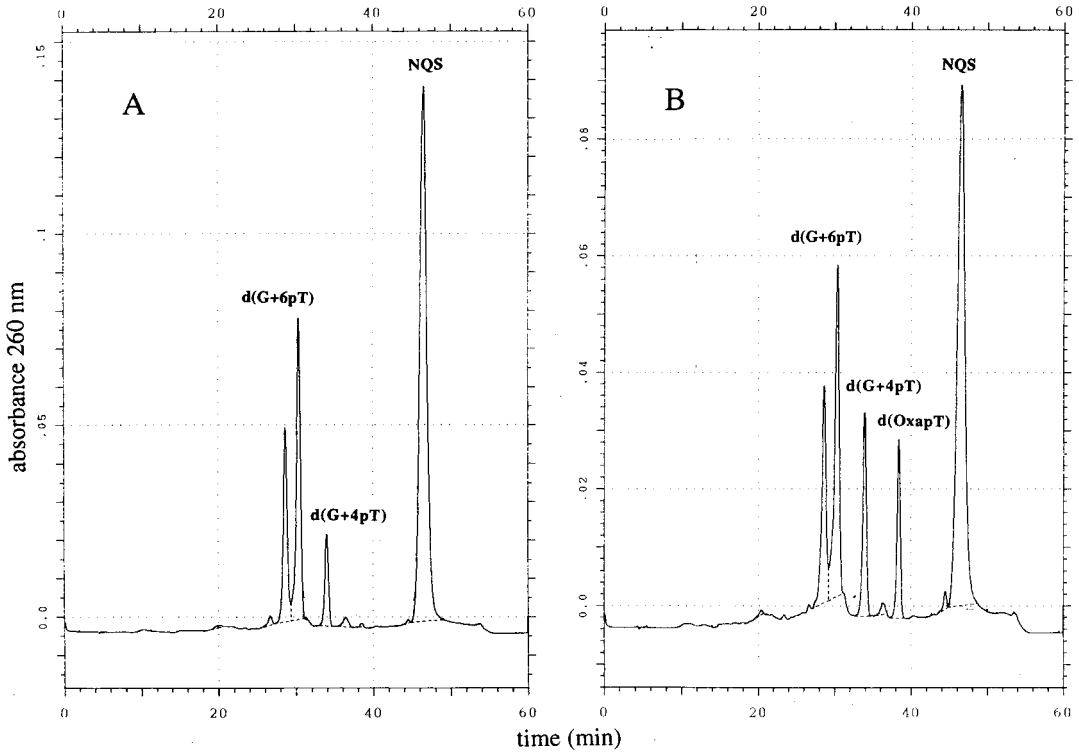


**Figure 4.** Reverse phase HPLC profiles of **d(G+6pT)** reoxidation in the presence of NQS after 5 min (A) or 30 min (B) at 65 °C. Formation of **d(G+4pT)** and **d(OxapT)**, its degradation product oxaluric acid derivative. Chromatogrphic conditions, gradient B.

**Table 2:** $^1$H NMR Data ($\delta$, ppm) for **d(G+6pT)** in DMSO-$d_6$; Chemical Shifts Were Measured from the Spectrum of a 35/65 Mixture of Minor and Major Isomers

| | deoxyribose | | | | | | | G+6 | | | thymine | | |
|---|---|---|---|---|---|---|---|---|---|---|---|---|---|
| | H1′ | H2′ H2″ | H3′ | H4′ | H5′ H5″ | 3′-OH | 5′-OH | H* | $NH_2$ C=NH[a] | NH7[b] | $CH_3$ | H6 | NH |
| **d(G+6pT)** major **G+6** | 5.76 | 2.03 2.12 | 4.51 | 3.80 | 3.39 | | 5.02 | 5.65 | 7.69 | 9.51 | | | |
| T | 6.21 | 2.04 2.08 | 4.27 | 3.86 | 3.80 | 5.41 | | | | | 1.80 | 7.76 | 11.28 |
| **d(G+6pT)** minor **G+6** | 5.53 | 2.41 2.12 | 4.51 | 3.79 | 3.39 | | 5.35 | 5.72 | 7.69 | 8.80 | | | |
| T | 6.21 | 2.04 2.08 | 4.27 | 3.86 | 3.80 | 5.41 | | | | | 1.81 | 7.79 | 11.28 |

[a] This signal accounts for 4 H. [b] One NH proton of **(G+6)** may not be detected.

another product with a *m*/*z* signal at 551 amu which was atributed to the "linear" oxaluric acid derivative described in section 3. The fragmentation at *m*/*z* = 436.3 amu may correspond to a 1′-amino-ribosyl residue. The total conversion of **d(G+6pT)** was achieved by the stepwise addition of an excess of NQS (30 equiv) during 3 h at 65 °C. It was noted that the two **d(G+6pT)** isomers were oxidized at similar rates since their HPLC peak ratio was constant. The heating of the mixture of the two **d(G+6pT)** isomers in water at 65 °C in the absence of NQS did not show any change in the HPLC chromatogram. We also performed control incubations showing that the reaction was not affected by anaerobic conditions or light. The **d(G+6pT)** derivatives were oxidized by electron transfer by NQS.

**6. NMR Analysis of d(G+6pT) Isomers. 6.1. Proton NMR.** The $^1$H NMR assignments were based on DQF-COSY and NOESY experiments. The $^1$H NMR spectra of the separately collected isomers of **d(G+6pT)** showed typically two families of resonances whose ratio was dependent upon which isolated compound was analyzed (data not shown). The two forms of **d(G+6pT)** derivatives could thus be distinguished by their different NMR spectra. The major resonances of the 35/65 (fast-/slow-eluting isomers) were attributed to the slow-eluting product, while the minor resonances were attributed to the fast-eluting one. The transformation of one isomer into the other did not occur in DMSO during the time course of the NMR analysis. The entire spectrum of **d(G+6pT)** isomers is shown in Figure S1 in the Supporting Information. As can be seen in Table 2 and in Figure S1, the $^1$H NMR spectrum of the equilibrium mixture containing a 35/65 (fast-/slow-eluting) ratio of **d(G+6pT)** isomers showed that some proton signals remained identical for both of them, whereas some others appeared as pairs of signals. The two singlets assigned to the H6 of thymine appeared at 7.79 ppm (minor, fast-eluting) and 7.76 ppm (major, slow-eluting) and gave together an integration accounting for one proton. A pair of two different resonances for the H1′ proton of the modified nucleoside moiety at 5.53 (minor, fast) and 5.76 (major, slow) were observed, whereas the H1′ signal of the thymidine nucleoside stayed unchanged at 6.21 ppm. The integration of the two resonances at 5.76 and 5.53 ppm accounted for one proton compared to the integration of the resonance of the H1′ proton of thymine at 6.21 ppm (one

proton). Two close but distinct sharp singlets for the methyl groups of thymine could also be detected at 1.80 and 1.81 for the slow- and fast-eluting isomers, respectively. Moreover, two new, singlet resonances appeared at 5.65 ppm (major isomer) and 5.72 ppm (minor one), both integrating for one proton. The corresponding proton, probably belonging to the modified base **(G+6)**, was referred to as H*. It must be noted that the chemical shifts of these singlets were slightly different depending on the water content in the NMR tube; 5.65 and 5.72 ppm values correspond to the spectrum shown in Figure S1 and described in Table 2. It was also possible to distinguish two different NMR resonances for broad signals of exchangeable protons such as the proton of the 5′-OH group at 5.02 and 5.35 ppm but also a NH-type proton of the **(G+6)** base moiety at 9.51 and 8.80 for the major and minor isomers, respectively (see Figure S1 and Table 2). We propose that this NH corresponds to the former NH at position 7 of guanine (Figure 1). A similar NH signal was described at 10.55 ppm on allantoin.[14] The relative integration of all these pairs of signals, the H*, the NH of the modified base, the H6 of T, the H1′, and the 5′-OH of **(G+6)**-modified sugar for the two isomers were in accordance with the ratio of isomers in different samples (data not shown). The sum of their integration accounted for one proton, and their integration ratio varied with the ratio of the two isomers in the sample.

The spectrum of **d(G+6pT)** compounds exhibited also a new broad resonance at 7.69 ppm. Its integration accounted for four protons. We tentatively attributed this signal to the protons of the guanidinium group of structure **4** (Figure 1). Thus the NH-type protons belonging to **(G+6)** base appeared as three signals: one broad signal at 7.69 ppm (4H) and a pair of very broad resonances at 9.51 and 8.80 ppm (1H). To slow the exchange processes we recorded an $^1$H NMR spectrum of the 35/65 mixture of isomers of **d(G+6pT)** in deuterated dimethylformamide. The decrease of the temperature from +20 to −10 °C (in DMF-$d_7$) resulted in the reduction of the width of the two signals corresponding to the pair of resonance of the NH of **(G+6)**, and the downfield displacement of their chemical shift due to a slowing of the exchange with water. At −20 °C the 9.51 and 8.80 ppm chemical shifts became 10.65 and 9.95 ppm, respectively. The signal for the NH of T moved in the same time from 11.28 to 12.05 ppm. A new resonance appeared during the process of the lowering of the temperature. It showed the same behavior as the above NH-type protons, reduction of width and downfield shift. At −10 °C it appeared at 9.20 ppm. This new signal was attributed to one NH of the guanidinium that may have been too broad or located under the broad resonance of the other guanidinium protons to be detected in DMSO at +20 °C. The temperature decrease promoted the splitting into two resonances of the signal corresponding to an integration of 4 protons of the **(G+6)** base (7.69 ppm in DMSO-$d_6$). These data show an intramolecular exchange between the protons of this signal that is consistent with a guanidinium group (structure **4** in Figure 1) although it was not possible to measure the integration values for all the NH resonances at −10 °C due to the close signal of DMF. When the temperature was lowered to −10 °C (in DMF-$d_7$) it was thus possible to observe five broad resonances for the NH-type protons of the **(G+6)** modified base at 10.65, 9.95 (1 NH-type proton, probably the former NH at position 7 of G, major and minor isomer of **(G+6)**, respectively), 9.20 (1 NH-type proton of **(G+6)**, probably the former NH at position 3 of G), 8.80 and 8.40 ppm (splitting of the guanidinium signal).

The $^1$H NMR spectrum of the 35/65 (fast-/slow-eluting) mixture of the two isomers of **d(G+6pT)** was also recorded in $D_2O$. This allowed us to detect the exchangeable protons of these compounds, namely, the protons of the modified base unit corresponding to the broad signals at 7.69, 8.80, and 9.51 ppm, the deoxyribose OH protons at 5.02, 5.35, and 5.41 ppm, and more importantly the new H* protons of the modified base unit corresponding to the two resonances at 5.65 and 5.72 ppm in DMSO-$d_6$. The $^1$H NMR of **d(G+6pT)** in $D_2O$ allowed us to monitor the slow exchange of the H* proton. After 1 h at room-temperature we observed 17% of exchange (integration 0.83 H), further heating of the sample at 37 °C for 1 h showed that the exchange reached 50%. The disappearance of the resonances of the two H* protons in $D_2O$ was complete after incubation of the sample overnight at room temperature (see Figure S3). The H* protons were tentatively attributed to the CH proton of the chiral carbon subjected to a keto−enol equilibrium. This point will be discussed later in the Discussion.

Some additional data concerning the differences between the two isomers were obtained from 2D DQF-COSY and NOESY experiments (through correlations with the two different H1′ signals). It was possible to observe that the major isomer of **d(G+6pT)** showed two close resonances for H2′ and H2″ protons (at 2.03 and 2.12 ppm, respectively), whereas the minor isomer showed two separate multiplets at 2.41 and at 2.12 ppm for H2′ and H2″, respectively. The assignment of H2′ and H2″ protons is based on the intensity of the NOESY correlation of these protons with H1′. The strongest correlation is the one between H1′ and H2″. NOESY correlations between the H1′ and H2′, H2″ protons are shown in Figure 5 (see also Figure S4). By comparing the DQF-COSY cross-peak intensities, the two coupling constants most sensitive to sugar pucker, $^3J$(H2″,H3′) and $^3J$(H3′,H4′), were estimated as being very weak (Figure S4). These data, associated to the relatively large trans coupling constants $^3J$(H1′,H2′), show that the two sugars of the dinucleotide derivative adopt mainly an (*S*)-type (C-2′ endo) puckered conformation in both isomers. The $^3J$(H1′,H2′) are equal to 9.70 or 8.60 Hz for the major or minor isomer of the **(G+6)** sugar, respectively, and 8.00 Hz for the thymidine sugar. The large downfield displacement of H2′ of the minor isomer may be explained by a significant change of the environment on the upper side of the sugar ring due to an inversion of configuration of the chiral center on the **(G+6)** base moiety.

From 2D NOESY experiments it was possible to find correlations between the protons of the H6 of thymine and all of the protons of its corresponding 2-deoxyribose moiety. Similarly, NOEs were observed between the proton H* of the modified **(G+6)** base moiety and the H1′, H2′, H2″ (Figure 5), and H3′ protons (Figure S5) of the 2-deoxyribose moiety of **(G+6)**. NOE between the H* and the H4′ of the **(G+6)** 2-deoxyribose was weaker (Figure S5). This was true for the major and the minor derivatives.

**6.2. Carbon NMR.** The assignment of the $^{13}$C resonance signals was initially based on literature data[13,14] and further confirmed by $^1$H−$^{13}$C heteronuclear scalar-correlated 2D NMR experiments (HMQC). Due to the overlapping of some resonances with those of the solvents, the $^{13}$C NMR spectra were recorded in DMSO-$d_6$ (see Figure S6) and DMF-$d_7$. These data are reported in Table 3 (DMSO) and Table S2 (DMF). The $^{13}$C NMR analyses were performed on a sample containing the 35/65 equilibrium mixture of both isomers. The assignment of

(13) Chang, C.-J.; DaSilva Gomes, J.; Byrn, S. R. *J. Org. Chem.* **1983**, *48*, 5151−5160.

(14) Poje, M.; Sokolic-Maravic, L. *Tetrahedron* **1986**, *42*, 747−751.

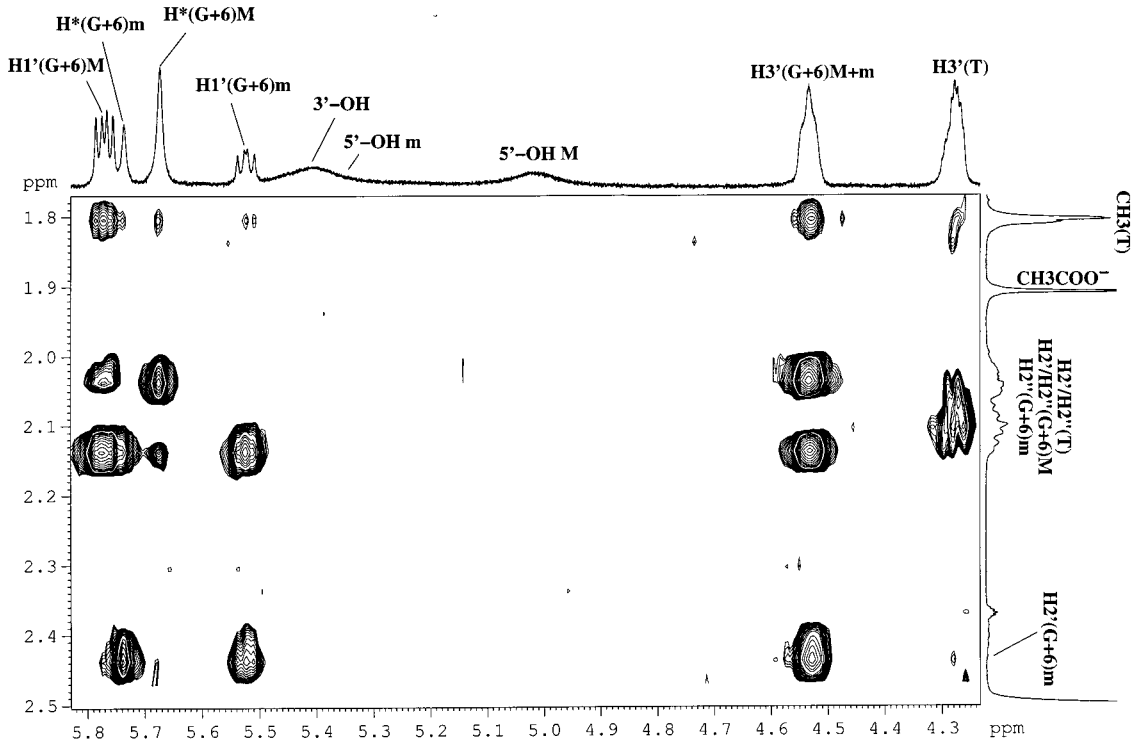


**Figure 5.** 2D $^1$H NOESY NMR spectrum showing correlations of protons of **d(G+6pT)** in DMSO-$d_6$. The signals of the major and minor isomer of **d(G+6pT)** are indicated by M and m, respectively.

**Table 3:** $^{13}$C NMR Data ($\delta$, ppm) for **d(G+6pT)** in DMSO-$d_6$

| | deoxyribose | | | | | (G+6) | | | | thymine | | | | |
|---|---|---|---|---|---|---|---|---|---|---|---|---|---|---|
| | C1′ | C2′ | C3′ | C4′ | C5′ | C* | NH$_2$ C=NH | NH CON | NH COC | $CH_3$ | C4 | C2 | C6 | C5 |
| **d(G+6pT)** major **G+6** | 82.2 | 35.5 | 75.7 | 85.6 | 62.9 | 63.3 | | 157.3 | 173.1 | | | | | |
| | | | $^2J$(C,P) 4.5 Hz | $^3J$(C,P) 5.2 Hz | | | | | | | | | | |
| T | 84.6 | 40 (under DMSO) | 71.8 | 86.6 $^3J$(C,P) 7.6 Hz | 65.6 | | | | | 12.9 | 164.7 | 151.4 | 136.9 | 110.7 |
| **d(G+6pT)** minor **G+6** | 82.7 | 36.2 | 75.9 $^2J$(C,P) 4.5 Hz | 85.6 $^3J$(C,P) 5.2 Hz | 63.0 | 64.9 | | 157.5 | 171.8 | | | | | |
| T | 84.6 | 40 (under DMSO) | 71.8 | 86.6 $^3J$(C,P) 7.6 Hz | 65.6 | | | | | 12.9 | 164.7 | 151.4 | 137.0 | 110.7 |

$^{13}$C carbon atoms of the sugar moieties resonances was deduced from HMQC experiment.

Concerning the carbon atoms belonging to the **(G+6)** base moieties, two resonances could be attributed to the two tertiary C* carbons of the two isomers of **(G+6)** base since they showed a clear correlation (HMQC) with the two corresponding H* signals. The major isomer C* at $\delta = 63.3$ ppm was connected to the H* of the major isomer at 5.65 ppm, whereas the C* of the minor one at $\delta = 64.9$ was correlated with the H* at 5.72. The intensity of the two $^{13}$C signals was in accordance with the ratio of the two isomers. Considering the 1D $^{13}$C spectrum, (Figure S6) the two isomers of **d(G+6pT)** showed clearly that the difference in the structure could be observed not only at the C* but also at carbons C1′, C2′, and C3′ of the **(G+6)** 2-deoxyribose since each of them appeared as pairs of signals (see Tables 3 and S2).

Heteronuclear $^1$H−$^{13}$C multiple bond correlation NMR spectroscopy (HMQC-LR, $J = 10$ Hz) (performed in DMSO-$d_6$) allowed the assignment of the C2 (151.4 ppm) and C6 (136.9 ppm) of thymine, taking into consideration the three-bond correlation with the H1′ of thymidine 2-deoxyribose. Similarly, the H1′ of the sugar, modified with **(G+6),** showed correlations with some carbons of the **(G+6)** base part. The H1′ proton of the major isomer of **(G+6)** at 5.76 ppm was connected through bonds with the major C* carbon at 63.3 (see Figure 6, upper part) and the H1′ proton of the minor isomer at 5.53 ppm with the minor C* carbon signal at 64.9 ppm (not shown). On the reverse, the C1′ carbon of thymidine unit was connected to the H6 of T (data not shown) and the C1′ of the **(G+6)** sugar (82.2 ppm) (see Figure 6, upper part) was found to be connected to the H* of the major isomer (5.65 ppm). These correlations were attributed to $^3J$(H,C). These attributions are particularly important since it allows the elimination of the structure proposed by Tannenbaum et al. for **d(G+6pT)** (**3** in Figure 1) with five bonds separating C* and the H1′ of the sugar.[11a]

From HMQC-LR data also, the H* proton of the major isomer at 5.65 ppm showed a correlation with a $^{13}$C signal at 157.3, and the H* proton of the minor isomer at 5.72 ppm was correlated with a $^{13}$C signal at 157.5 ($^3J$(H*,C) in Figure 6, lower part). We propose that the carbon atom of the modified base **(G+6)** which appeared at two different chemical shifts, depending on the isomer, corresponds to the NH(CO)N carbon of the five-membered ring, namely the former C8 of the initial guanine.

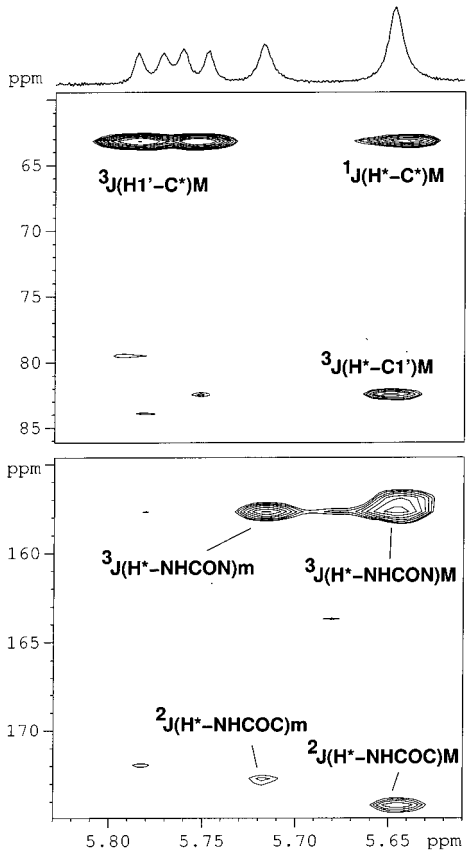


**Figure 6.** Heteronuclear $^1$H−$^{13}$C multiple bond correlation NMR spectrum (HMQC-LR, $J$ = 10 Hz) (performed in DMSO-$d_6$) of **d(G+6pT)**. M, refers to the major and m, to the minor isomer of **d(G+6pT)**.

Moreover, the H* proton at 5.67 ppm of the major isomer was correlated not only with C8 at 157.3 ppm as mentioned above but also to a carbon resonance at 173.1 ppm (see $^3J$(H*,C), Figure 6, lower part). The H* resonance of the minor isomer at 5.73 ppm was also found to be correlated to a carbon resonance at 171.8 (see $^2J$(H*,C) in Figure 6, lower part). This carbon resonance was tentatively attributed to the NH(CO)C*, the former C5 of the initial guanine. The fourth carbon of the **(G+6)** base moiety (guanidinium carbon, former C2 of G) was not observed. This may be explained by the fact that this resonance may be very broad due to strong quadrupole effects of three N nuclei linked to this carbon, together with the low amount of material available for analysis.

The $^{13}$C spectrum of **d(G+6pT)** confirmed the dinucleoside monophosphate structure of compound **4** by the coupling of the sugar carbons with the phosphorus atom (see Table 3).

**6.3. Phosphorus NMR.** The $^{31}$P NMR spectrum, in DMSO-$d_6$, for the 35/65 mixture of **d(G+6pT)** isomers, showed two singlets corresponding to the phosphorus atom of each isomer at 2.18 and 2.07 ppm for the major and minor isomer, respectively.

## Discussion

The oxidation of the dinucleoside monophosphate **d(GpT)** by Mn−TMPyP/$KHSO_5$ gave two products **d(IzpT)** and **d(G+4pT)** (**1**, Figure 1). While the guanine oxidation modified residue **(G+4)** was the major product of oxidation in the case of double-stranded oligonucleotides, the major product was **d(IzpT)** in the case of **d(GpT)**. Since **d(G+4pT)** is not a precursor of **d(IzpT)**, it might be proposed that oxidation at C8 of guanine precludes the formation of imidazolone. The oxidation at C8 of guanine may be favored in double-stranded DNA structures compared to simplified models such as dinucleoside monophosphates. A competition between the oxidation of C8 and an intramolecular cyclization leading to imidazolone (attack of the guanidinium amino group onto the C5, followed by the loss of formamide)[10] would be at the origin of differences in the ratio of these two reaction products. The attack rate of the guanidinium amino group onto the C5 is probably reduced when the guanidinium in engaged in hydrogen bonds in double-stranded DNA.

It was, however, possible to collect the **d(G+4pT)** product on a large scale in order to establish its structure by NMR data. Since **1** was not stable enough under the conditions used for its isolation, this compound was transformed into a stable derivative by reduction with $NaBH_4$. The reduction gave rise to two **d(G+6pT)** isomers (**4**, Figure 1). The **d(G+6pT)** compounds were stable during the purification procedure and could be analyzed by NMR as well as by mass ESI/MS. The $NaBH_4$ reduction of the imine function present on the **(G+4)** structure creates a new chiral center with formation of two *R* and *S* enantiomers on the **(G+6)** moiety; one should then expect two diastereoisomers for **d(G+6pT)**.

Among the three proposed structures in Figure 1 for the **d(G+4pT)** and for the corresponding reduced **d(G+6pT)** compounds, **3** (**6** when reduced) can be discarded from NMR HMQC-LR data. It was found that the C* carbon of the **(G+6)** base moiety was connected through bonds to the H1′ of the sugar carrying the modified base. The H* proton of the (G+6) base moiety was also connected to the C1′ carbon of the sugar. These cross-peaks corresponded to $^3J$(C,H) coupling constants. The structure **3** (**6** when reduced) shows five bonds between these atoms and thus cannot fit with the observed correlations.

The structure of **d(G+4pT)** could be **1** or **2**. The two isomers of the reduced product, **d(G+6pT)**, gave a fragmentation product upon LC-ESI/MS analyses, corresponding to the loss of the guanidinium moiety. Structure **5** is not compatible with a loss of such a fragment during MS analyses. We thus propose that the two **d(G+6pT)** compounds correspond to the two diastereoisomers of **4**. Consequently, structure of **d(G+4pT)** is proposed to be **1**. Structure **2** is not compatible with the structure of oxaluric acid which would arise from the hydrolysis of **d(G+4pT)** (**2**) upon heating (this work). Neither is it compatible with the structure of "linear" oxaluric acid derivative which arises from a **(G+4)** lesion generated by oxidation of 8-oxo-7,8-dihydroguanine by singlet oxygen[12] analyzed by ESI/MS/MS or with the structure of oxaluric acid obtained from the hydrolysis of the nitration product of 8-oxo-7,8-dihydro-2′-deoxyguanosine under oxidation by peroxynitrite[11b] analyzed by NMR with the two NH protons described at 8.87 and 7.04 ppm (DMSO-$d_6$); the former showed a coupling constant with the H1′ of the sugar carrying the modified residue.

The relative stability of **1** in the oxidizing reaction medium can be understood from literature data (Figure 7). Poje et al.[14] reported the oxidation of urate and *N*-1-methyl-urate under two types of oxidizing conditions. Under strong oxidizing conditions, compounds reminiscent of dehydro-guanidinohydantoin residue, dehydro-allantoin, **7a** or the corresponding methylated derivative **7b**, were isolated, depending on the starting urate derivative. Compound **8** was not formed when compound **7b** was observed. Acid hydrolysis of compound **7a** led to parabanic acid and urea (Figure 8). When the starting urate was $^{14}$C-labeled at the C2, the label was found entirely on urea and not on parabanic acid. Consequently, an equilibrium between **1** and **2** through a bicyclic

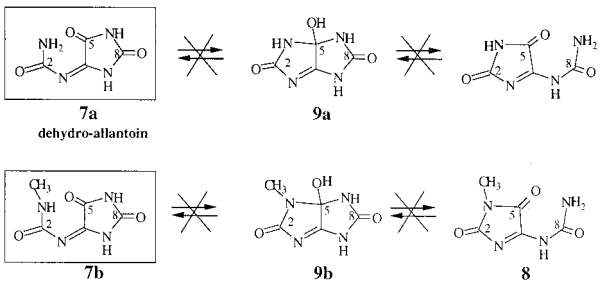


**Figure 7.** Stability of dehydro-allantoin.[14] No interconversion between **1** and **2**. Boxes refer to isolated products.

intermediate like **9** can be excluded (Figure 7), since neither **7a** nor **7b** undergoes an equilibrium through **9a** or **9b**, respectively. The structure **1** proposed for **d(G+4pT)** should be stable under the reaction conditions used in the present work.

However, after the reduction of the imine function at the C4−N3 bond, an equilibrium between the two structurally different species due to the opening of a dissymmetric bicyclic intermediate might be possible. A bicyclic compound **10** was postulated to explain the isomerization of allantoin (Figure 9A). The $KMnO_4$ degradation of the $^{14}C-C2$- and the $^{14}C-C8$-labeled uric acid led to a mixture of equally labeled allantoins (Figure 9B).[15] The reduction products of **1**, **d(G+6pT) 4**, might be prone to a similar equilibrium through the formation of intermediate **11** giving rise to **5** (Figure 10). In the case of dissymmetric derivatives, with *N*-methyl groups, the opening of this bicyclic intermediate was shown, however, to occur on the side which gives the more stable product, that is the one that carries the substituted nitrogen within the cycle. Upon low oxidation conditions of *N*-1-methyl urate derivative, Poje et al.[14] reported that **12** was obtained and was not subjected to isomerization (Figure 11). A related important work on urate oxidation concerns various *N*-methylated urate substrates which give also methylated allantoins.[15] The authors concluded that the equilibrium involving a bicyclic dissymmetric intermediate (reminiscent of **10** for allantoin or **13** for *N*-methylated derivative) is always displaced toward the opening on the nonmethylated side.[15] According to these previous works, **4** should be a favored structure compared to **5** due to the presence of the sugar on the N9 of G. This is exactly what was observed in the present work. We propose that the guanine oxidation product, **4**, has a dehydro-guanidinohydantoin structure similar to that observed in urate oxidation.

The isomerization of the two diastereoisomers of **d(G+6pT)** may be due to a keto−enol equilibrium (C4−C5 bond) with one of the two forms, *R* or *S*, being slightly thermodynamically favored over the other. The $^1H$ NMR analysis in $D_2O$ confirmed that the H* protons of both **d(G+6pT)** isomers exchanged with water indicating the possible keto−enol equilibrium. The timescale of hydrogen exchange in $D_2O$ (hours) is compatible with that of the equilibrium observed upon tentative isolation of separated **d(G+6pT)** isomers. The equilibrium between **4** and **5** would not be correlated to an exchangeable H* proton although a keto−enol equilibrium is also possible for stuctures **4** and **5**.

The $^1H$ NMR analyses in DMSO-$d_6$ or in DMF-$d_7$ of the sample consisting of a mixture of the two isomers of **d(G+6pT)** were also consistent with structure **4**.

The **(G+4)** residue studied in this work is not a precursor of the imidazolone (Iz)-modified base since we never observed the transformation of **d(G+4pT)** to **d(IzpT)**. The formation of the dehydro-guanidinohydantoin should be considered as an independent route in guanine oxidation, compared to the one leading to imidazole.

The guanidinohydantoin **(G+6)**, can also be observed in guanine oxidation, as previously proposed in the oxidation of 7,8-dihydro-8-oxo-2′-deoxyguanosine[16] or of guanine within a DNA duplex,[17] but the structure of **(G+6)** was not firmly established.

## Conclusions

A guanine oxidation product **(G+4)** was observed in the oxidation of a dinucleoside monophosphate **d(GpT)** by the Mn−TMPyP/$KHSO_5$ system. From mass data obtained with its hydrolysis product, an oxaluric acid derivative, and from mass and NMR data obtained with its reduced form **(G+6)**, we propose that the **(G+4)** lesion corresponds to a dehydro-guanidinohydantoin structure, less stable than the guanidinohydantoin **(G+6)** obtained by $NaBH_4$ reduction of **(G+4)**. The present work performed with a dinucleotide can be considered as an important step to confirm the identification of such lesion at the level of double-stranded DNA.

## Experimental Section

**Materials.** Thymidine-5′-monophosphate and 1,2-naphthoquinone-4-sulfonate, sodium salt were purchased from Sigma-Aldrich. Potassium monopersulfate, $KHSO_5$ (triple salt 2 $KHSO_5 \cdot K_2SO_4 \cdot KHSO_4$, Curox) was from Interox, piperidine from Fluka. Mn−TMPyP was prepared as previously described.[18]

**Nuclear Magnetic Resonance.** NMR spectra were recorded on a Bruker AMX400 spectrometer equipped with a 5 mm triple resonance inverse probe with dedicated $^{31}P$ channel operating at 400.13 MHz for $^1H$, 161.97 MHz for $^{31}P$, and 100.61 MHz for $^{13}C$. All chemical shifts for $^1H$ and $^{13}C$ are relative to TMS using $^1H$ (residual) or $^{13}C$ chemical shifts of the solvent as a secondary standard.[31]P chemical shifts were referenced to an external 85% $H_3PO_4$ sample. $^1H$ and $^{13}C-\{1H\}$ spectra were recorded at 293 K in DMSO-$d_6$ and DMF-$d_7$. $^{31}P-\{1H\}$spectrum was acquired at 293 K in DMSO-$d_6$. $^1H$ 1D experiments were acquired at several time intervals after dissolution of the sample in $D_2O$ to monitor the hydrogen−deuterium exchanges. Temperature calibration was determined using a methanol chemical shift thermometer.

$^1H$ NMR spectra were recorded at 293, 283, 273, 263, 253, and 233 K in DMF. 30 s relaxation delays were used to obtain reliable integration data. All 2D experiments were acquired at 293 K.

Gradient-enhanced $^1H$ DQF-COSY included 96 scans per increment. $^1H-^{13}C$ correlation spectra using a gradient-enhanced HMQC sequence (delay was optimized for $^1JCH$ of 135 Hz) was obtained with 256 scans per increment in DMF-$d_7$. A gradient-enhanced HMQC-LR experiment was performed allowing 50 ms for long-range coupling evolution (368 scans were accumulated) in DMSO-$d_6$. Typically, 2048 $t_2$ data points were collected for 256 $t_1$ increments.

A standard two-dimensional $^1H$ NOESY experiment (mixing time of 250 ms) was acquired in a phase-sensitive mode. Eighty scans for each of the 256 $t_1$ values were collected with 4096 points.

**Synthesis of the Dinucleoside Monophosphate, d(GpT). d(GpT)** was synthesized by a modified phosphotriester approach with the use of 4-methoxypyridine *N*-oxide as nucleophilic catalyst of internucleotide coupling reaction.[19] Starting nucleotide and nucleoside components, 5′-*O*-dimethoxytrityl-2-*N*-isobuturyl-2′-deoxyguanosine, 3′-*O*-(2-chlorophenyl)phosphate and 3′-*O*-benzoylthymidine, respectively, were

(15) Abblard, J.; Meynaud, A.; Definod, G. *Bull. Soc. Chim. Fr.* **1971**, *3*, 942−946 and references therein.

(16) Duarte, V.; Muller, J. G.; Burrows, C. J. *Nucleic Acids Res.* **1999**, *27*, 496−502.

(17) Stemmler, A. J.; Burrows, C. J. *J. Am. Chem. Soc.* **1999**, *121*, 6956−6957.

(18) Bernadou, J.; Pratviel, G.; Bennis, F.; Girardet, M.; Meunier, B. *Biochemistry* **1989**, *28*, 7268−7275.

(19) Efimov, V. A.; Chakhmakhcheva, O. G.; Ovchinnikov, Y. A.; *Nucleic Acids Res.* **1985**, *13*, 3651−3666.

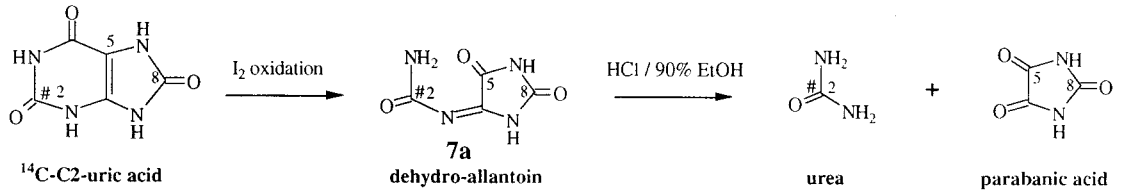


**Figure 8.** Acid hydrolysis of dehydro-allantoin into parabanic acid and urea.[14] In the present case, # indicates a $^{14}$C-labeled carbon atom.

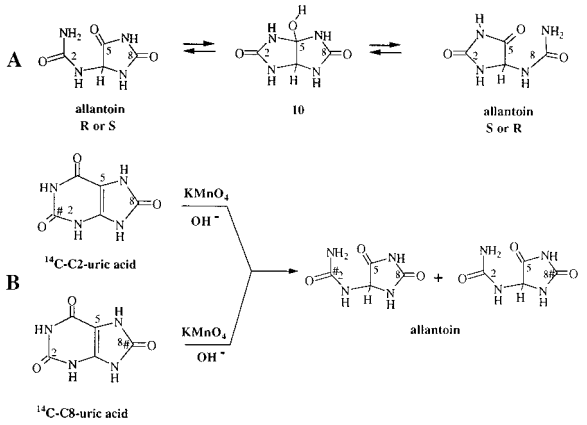


**Figure 9.** (A): allantoin, a symmetrical bicyclic intermediate is formed in solution.[15] (B): oxidation of $^{14}$C-labeled uric acid at C2 or C8 into allantoin.[15] The # indicates a $^{14}$C-labeled carbon atom.

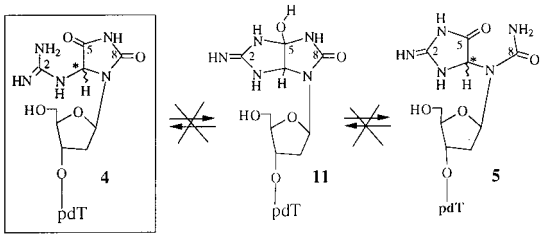


**Figure 10.** Interconversion between **4** and **5** was not observed.

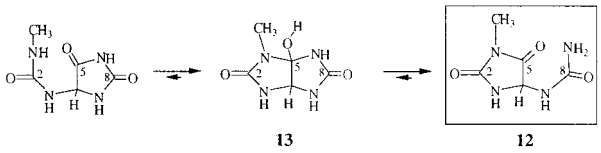


**Figure 11.** Opening of dissymmetric bicyclic intermediate (**13**) on the nonmethylated side.[14,15] Box shows isolated product.

prepared by usual procedures.[20] After standard deprotection, final dinucleotide was purified by column chromatography on DEAE-Sephadex in the gradient 0.05−0.25M triethylammonium bicarbonate, pH 7.5, and 180 mg of **d(GpT)** was obtained. The absorption coefficient of **d(GpT)** was $10 \times 10^3$ $M^{-1}$ $cm^{-1}$ at 260 nm.

**HPLC and HPLC-ESI/MS Analysis.** The HPLC analysis of the samples was done on a reverse-phase column (Nucleosil C18, 10 $\mu$m 250 × 4.6 mm from Interchrom, France), eluted with a linear gradient for 1 h, at 1 mL/min. The eluents were A = 10 mM TEAA pH 6.5, B = 20% $CH_3CN$ in 10 mM TEAA pH 6,5. Two types of gradients were used, gradient A: from 0 to 20% of $CH_3CN$ or gradient B: from 1 to 10% $CH_3CN$. A diode array detector (Waters) allowed the detection of the products ($\lambda$ = 260 nm) and the monitoring of their UV−vis spectra. The on-line ESI/MS spectrometer was a Perkin-Elmer SCIEX API 365 used in the negative mode.

**Preparative HPLC.** The isolation of the oxidation products of **d(GpT)** was done (from the preparative reaction medium described below) by collection of the products eluted from a reverse phase semipreparative column (Nucleosil C18, 10 $\mu$m, 250 × 6.2 mm from Interchrom, France) eluted in a gradient mode at 2 mL/min. The gradient was from 1 to 20% of $CH_3CN$ for 1 h by combination of the two eluents, solvent A = 10 mM TEAA pH 6.5, solvent B = solvent A containing 20% of $CH_3CN$. The detection was at 260 nm. Total reaction volume (2 mL) was injected directly.

**Analytical Oxidation of d(GpT) by Mn−TMPyP/$KHSO_5$.** The dinucleoside monophosphate, **d(GpT)**, (500 $\mu$M) was incubated at 0 °C in triethylammonium acetate (TEAA) buffer pH 6.5 (20 mM) with Mn−TMPyP (2 $\mu$M). After preincubation (15 min), $KHSO_5$ (0.5 mM) was added. Final volume was 100 $\mu$L, final concentrations are indicated in parentheses. After 5 min of reaction at 0 °C, the reaction was stopped by the addition of HEPES buffer pH 8 (100 mM), and then injected for HPLC-ESI/MS analysis with gradient program A. The retention times of **d(GpT)**, **d(IzpT)**, and **d(G+4pT)** were 30.9, 26.8, and 23.5 min, respectively, under these conditions.

**Preparative Oxidation of d(GpT) by Mn−TMPyP/$KHSO_5$ and Isolation of d(G+6pT) Products.** The starting dinucleoside monophosphate, **d(GpT)** (3 mM, 3.4 mg) was incubated with Mn−TMPyP (16 $\mu$M) and $KHSO_5$ (3.5 mM) in 80 mM TEAA buffer pH 6.5, at 0 °C during 10 min. The final concentrations are indicated. The total reaction volume was 1.9 mL. The reaction was stopped by the addition of HEPES buffer pH 8 (35 mM), and the products were separated by semipreparative HPLC. This individual reaction was repeated 18 times to obtain enough material. The collected **d(G+4pT)** fractions were pooled together, and 10 $\mu$L of 1 M $NaBH_4$ solution was added per each mL of collect to reduce the oxidized guanidinohydantoin before freezing and lyophylization. The reduction was carried out during 30 min at ambient temperature and stopped by the addition of 20 $\mu$L of acetone per each 10 $\mu$L of $NaBH_4$ solution added. The pooled fractions were evaporated to dryness and purified again onto the semipreparative HPLC column to remove the salts from the reduction medium. The two products of reduction were collected separately, freezed and lyophylized again. The dry samples were then dissolved in 0.5 mL of NMR solvent.

**Piperidine Treatment of d(G+6pT).** A dry aliquot of **d(G+6pT)** sample (0.3 OD at 260 nm) was dissolved in 200 $\mu$L of 1 M piperidine and heated at 90 °C for 30 min. The piperidine solution was lyophylized, and the sample was washed twice with 100 $\mu$L of Milli-Q water followed by lyophylization and dissolved in water for HPLC analysis.

**Reoxidation of d(G+6pT).** Purified **d(G+6pT)** (100 $\mu$M) was incubated with 1,2-naphthoquinone-4-sulfonate (200 $\mu$M) in water at room temperature or at 65 °C. To estimate the concentration of **d(G+6pT)**, the $\epsilon$ value of **d(G+6pT)** at 260 nm was taken as the $\epsilon$ value of thymidine, 9700 $M^{-1}$ $cm^{-1}$. The reaction was monitored by HPLC or HPLC-ESI/MS with gradient program B. The detection of the products of the reaction was at 260 nm (and at 355 nm for NQS).

**Acknowledgment.** A.C. received a fellowship from a joint program between the LCC (Toulouse, France) and the CMMS (Lodz, Poland). I.D. is grateful to the University Paul Sabatier (Toulouse) for a fellowship. Professors Jean Bernadou (LCC, Toulouse) and Cynthia Burrows (University of Utah) are acknowledged for fruitful discussions. HPLC-ESI/MS data were obtained from the "Service de Spectrométrie de Masse de l'Université Paul Sabatier, Toulouse, FR14-LCC-CNRS" operated by Suzy Richelme and Catherine Claparols.

**Supporting Information Available:** Table S1: $^1$H NMR data ($\delta$, ppm) for **d(IzpT)** in DMSO-$d_6$; Table S2: $^{13}$C NMR data ($\delta$, ppm) for **d(G+6pT)** in DMF-$d_7$; Figure S1: $^1$H NMR

(20) *Oligonucleotide synthesis: a practical approach*; Gait, M. J., Ed.; Oxford University Press: Oxford, New York, Tokyo, 1984.

spectrum of a 35/65 mixture of **d(G+6pT)** isomers in DMSO-$d_6$; Figure S2: ESI/MS/MS fragmentation of **d(G-19pT)** compound obtained from the degradation of **d(G+4pT)**; observed *m*/*z* signals from the fragmentation of the parent monocharged $[M - H]^-$ ion ($m/z = 551$); Figure S3: NMR spectra of **d(G+6pT)** isomers in $D_2O$ showing the exchange of the H* proton; the signals of the major and minor isomer of **d(G+6pT)** are indicated by M and m, respectively; Figure S4: H1′−H3′ to H2′, 2″-H4′ region of the DQF-COSY spectrum of a 35/65 mixture of **d(G+6pT)** isomers in DMSO-$d_6$; the signals of the major and minor isomer of **d(G+6pT)** are indicated by M and m, respectively; Figure S5: H1′, H* to H3′, H4′ region of the $^1$H NOESY spectrum of **d(G+6pT)** in DMSO-$d_6$; the signals of the major and minor isomer of **d(G+6pT)** are indicated by M and m, respectively; the intensity of the cross-peak between H1′ and H4′ is stronger than the one between the H1′ and H3′ for the protons of the three types of sugars ($\beta$-furanose configuration); Figure S6: $^{13}$C NMR spectrum of a 35/65 mixture of **d(G+6pT)** in DMSO-$d_6$ (PDF). This material is available free of charge via the Internet at http://pubs.acs.org.

## Abbreviations

amu, atomic mass unit; TEAA, triethylammonium acetate; Mn-TMPyP, manganese(III)-bis-aqua-*meso*-tetrakis(4-*N*-methylpyridiniumyl)-porphyrin; OD, optical density at 260 nm; T, thymine; G, guanine; ESI/MS, electrospray ionization mass spectrometry; NQS, 1,2-naphthoquinone-4-sulfonate; HMQC-LR, heteronuclear $^1$H−$^{13}$C multiple quantum coherence-long-range NMR spectroscopy; NOESY, nuclear Overhauser enhancement spectroscopy; DQF-COSY, double quantum filtered correlation spectroscopy; TMS, tetramethylsilane.

JA003945P